
Lenka RANDÝSKOVÁ¹, Petr JANAS²**NON-LINEAR SOLUTION OF STEEL ARC REINFORCEMENT
WITH INFLUENCE OF PASSIVE FORCES****NELINEÁRNÍ ŘEŠENÍ OCELOVÉ OBLOUKOVÉ VÝZTUŽE PŘI EXISTENCI PASIVNÍCH SIL****Abstract**

Geometrically and physically non-linear solution of steel arc reinforcement with influence of passive forces is presented in this paper. The Winkler model is used to the solution. It is an elastic one-parametrical model, which is characterized by the only one constant C . A displacement method is utilized along with an iterative procedure. The software was created, which is based on derived procedure. An example was solved consequently.

Keywords

Non-linear solution, arc reinforcement, Winkler model, displacement method.

Abstrakt

Článek se zabývá geometricky a fyzikálně nelineárním řešením ocelové obloukové výztuže. Při řešení se počítá s interakcí výztuže a okolní horniny. Je použit Winklerův jedno-parametrický model. Základem celého řešení je obecná deformační metoda a iterační postup výpočtu. Odvozený postup byl podkladem pro sestavení softwaru v prostředí Microsoft Excel a Visuál Basic, který byl následně použit k řešení příkladu.

Klíčová slova

Nelineární řešení, oblouková výztuž, Winklerův model, obecná deformační metoda.

1 INTRODUCTION

A steel reinforcement consisting of circular arcs plays an important role as a reinforcing element in the mining industry and is used frequently in underground building processes. The processes under the ground are, in contrast to the building process above the ground, often exposed to extensive deformation. Consequently, when statically analyzing the reinforcement, attention should be paid to both the geometrical and physical non-linearities.

The loading of steel reinforcements in long mining works can be, in principle, active or passive. The active load is the result of weight of loose ground which affects the reinforcement in the vertical and horizontal directions. It can also develop from the weight of the technology plant or because of a one-off load which appears during shock bumps. In the long mine workings, the active load can result from active deformation of a rock mass subject to deformation.

¹ Ing. Lenka Randýsková, Department of Structural Mechanics, Faculty of Civil Engineering, Technical University of Ostrava, Ludvíka Podéště 1875/17, 708 33 Ostrava - Poruba, phone: (+420)597321919, e-mail: lenka.randyskova@vsb.cz.

² Doc. Ing. Petr Janas, CSc., Department of Structural Mechanics, Faculty of Civil Engineering, Technical University of Ostrava, Ludvíka Podéště 1875/17, 708 33 Ostrava - Poruba, phone: (+420)597321308, e-mail: petr.janas@vsb.cz.

The active loading causes the steel arc reinforcement to deform. If the steel arc reinforcement is in contact with the rock and the reinforcement starts distorting “towards” the rock mass”, the rock mass affects the reinforcement which starts, in turn, deforming. Such induced forces are referred to as the passive forces and the load is referred to as a passive load. This means, the passive load is deformation caused by active loads of steel arc reinforcement.

The passive forces typically influence very positively the load-carrying capacity of the steel arc support. They stabilize the steel arc support by inducing more positive components of the internal forces that are those typical of the active load. [1]

2 SOLUTION

Let us assume a reinforcement which is subject to active loads. Consequently, the reinforcement starts deforming and, if in contact with the rock and if deforms “towards” the rock, passive forces will appear there. The both conditions above, this means the rock contact and deformation direction, need to be fulfilled. Otherwise, the passive forces will not be created.

First, let us assume that the passive forces will appear along the perimeter of the reinforcement. Let us divide the entire length of the arc into n segments with the ds_i . Let us also assume that in each joint, the passive force affects perpendicularly the central line of the arc. Each passive force represents another simple link – a kind of an elastic flexible hinged rod. (Note: The oldest and simplest interaction model was used for the solution – the Winkler model. This basic model ranks among single-parametric models with a linear response to the load. This means, to describe it, a single constant is necessary: the soil compressibility coefficient (C).

One obtains n straight-line segments forming the arc and $n-1$ hinged rods which equivalently replace the produced passive forces (Fig. 1). This distribution results in n_p unknown parameters in the $\{r\}$ deformation vector. The unknown deformation can be obtained using the general deformation method [2] and solving the following system of equations.

$$[K] \cdot \{r\} = \{F\}, \quad (1)$$

where $[K]$ is the total rigidity matrix and $\{F\}$ is the system loading vector.

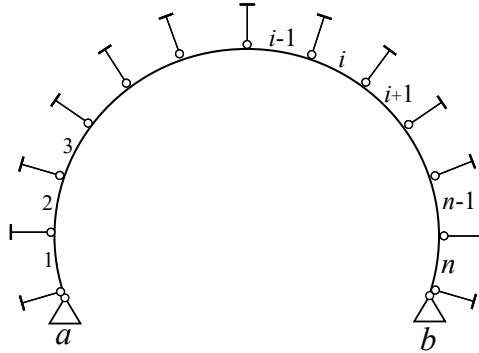


Fig. 1: Pattern of the arc, if the passive forces exist

During the loading, the material does not behave linearly after the ultimate strength is exceeded - the material behaves in a physically non-linear way. The shape of its profile may change as well – see Fig. 6. The reason is changes in the bending rigidity of the profile where such changes depend on internal forces (on the bending moment M and on normal forces N). The bending rigidity for certain components of the internal forces is regarded as linear (the equivalent bending rigidity). In order to express it unambiguously, it is advisable to define the bending rigidity as a function of relative angular displacement and direct force [5], see Fig. 2.

2.1 Rigidity matrix of the system, K

The total rigidity matrix, $[K]$, is obtained by localization of the global rigidity matrixes of the individual arc segments and rigidity matrices of the hinged rods which simulate the passive forces. In case of a non-linear solution, the matrix, $[K]$, is the function of the loading vector, $\{F\}$.

The global rigidity matrix, $\{k_i\}$, of the individual straight-line segments, which form the arc reinforcement, is obtained by (2), (3) a (4). [3]

$$[k_i^*] = \begin{bmatrix} \frac{EA}{ds_i} & 0 & 0 & -\frac{EA}{ds_i} & 0 & 0 \\ 0 & \frac{12EI_i}{ds_i^3} & -\frac{6EI_i}{ds_i^2} & 0 & -\frac{12EI_i}{ds_i^3} & -\frac{6EI_i}{ds_i^2} \\ 0 & -\frac{6EI_i}{ds_i^2} & \frac{4EI_i}{ds_i} & 0 & \frac{6EI_i}{ds_i^2} & \frac{2EI_i}{ds_i} \\ -\frac{EA}{ds_i} & 0 & 0 & \frac{EA}{ds_i} & 0 & 0 \\ 0 & -\frac{12EI_i}{ds_i^3} & \frac{6EI_i}{ds_i^2} & 0 & \frac{12EI_i}{ds_i^3} & \frac{6EI_i}{ds_i^2} \\ 0 & -\frac{6EI_i}{ds_i^2} & \frac{2EI_i}{ds_i} & 0 & \frac{6EI_i}{ds_i^2} & \frac{4EI_i}{ds_i} \end{bmatrix} \quad (2)$$

$$[T_i] = \begin{bmatrix} \cos\psi_i & \sin\psi_i & 0 & 0 & 0 & 0 \\ -\sin\psi_i & \cos\psi_i & 0 & 0 & 0 & 0 \\ 0 & 0 & 1 & 0 & 0 & 0 \\ 0 & 0 & 0 & \cos\psi_i & \sin\psi_i & 0 \\ 0 & 0 & 0 & -\sin\psi_i & \cos\psi_i & 0 \\ 0 & 0 & 0 & 0 & 0 & 1 \end{bmatrix} \quad (3)$$

$$[k_i] = [T_i]^T \cdot [k_i^*] \cdot [T_i] \quad (4)$$

ds_i is there the length of the individual arc segments and ψ_i is the displacement angle of the i^{th} segment. EI_i is the equivalent bending rigidity of the segment, which, during the calculation, is obtained by linear interpolation depending on the relative angular displacement of the segment, $d\varphi_i$, and direct force, N_i , from the curves in Fig. 2. [4]

$$d\varphi_i = \left| \frac{1}{ds_i} (\varphi_i - \varphi_{i-1}) \right| \quad (5)$$

$$\{R_i^*\} = [T_i] \cdot [k_i] \cdot \{r_i\} \quad (6)$$

$$N_i = -R_{i,1}^* = R_{i,4}^* \quad (7)$$

$\{r_i\}$ – is the global strain vector for the i^{th} segment

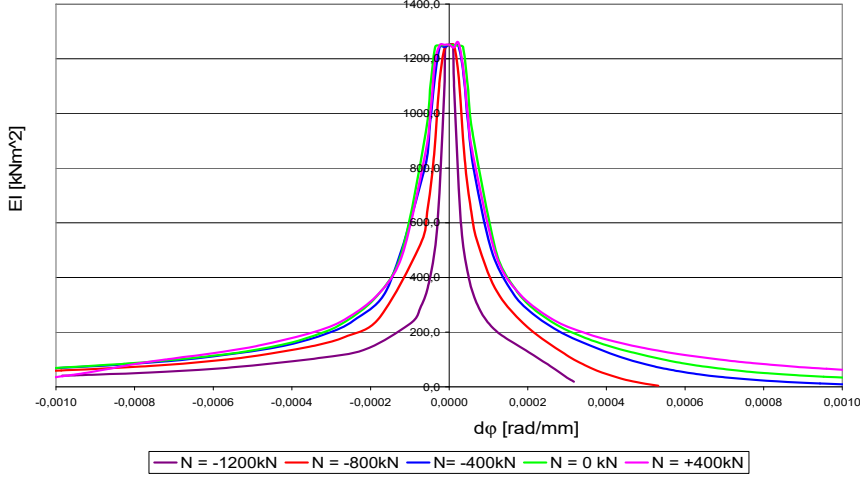
$\{R_i^*\}$ – is the local vector of end forces for the i^{th} segment

$$\begin{aligned} d\varphi_i \geq d\varphi_{m,j-1} \cap d\varphi_i < d\varphi_{m,j} &\Rightarrow \\ \Rightarrow \tilde{EI}_{m,i} = EI_{m,j-1} - \frac{(d\varphi_i - d\varphi_{m,j-1})}{(d\varphi_{m,j} - d\varphi_{m,j-1})} (EI_{m,j-1} - EI_{m,j}) &\quad (8) \end{aligned}$$

$$\begin{aligned}
N_i \geq N_m \cap N_i < N_{m+1} &\Rightarrow \\
\Rightarrow EI_i = E\tilde{I}_{m,i} - \frac{(N_i - N_m)}{(N_{m+1} - N_m)}(E\tilde{I}_{m,i} - E\tilde{I}_{m+1,i}) &\quad (9)
\end{aligned}$$

Fig. 2: Curves of the equivalent bending rigidity, EI , for the profile P-28

The global rigidity matrix, $\{k_i\}$, of the hinged rods which is the equivalent replacement of the passive forces is obtained using the formulae below. For the hinged rods, the length $l=l$ is chosen. The surface is the profile width, b , (for P-28, $b = 150$ mm) multiplied with the sum of the halves of



the length, ds , of the two adjacent arc segments. The modulus of elasticity, E , is given by the compressibility coefficient, C .

Fig. 3: Detail of the rods in the i^{th} joint incl. the strain

$$[k_i^*] = \begin{bmatrix} 0 & 0 & 0 & 0 & 0 & 0 \\ 0 & 0 & 0 & 0 & 0 & 0 \\ 0 & 0 & 0 & 0 & 0 & 0 \\ 0 & 0 & 0 & K_{podl,i} & 0 & 0 \\ 0 & 0 & 0 & 0 & 0 & 0 \\ 0 & 0 & 0 & 0 & 0 & 0 \end{bmatrix} \quad (10)$$

$$K_{podl,i} = \frac{EA}{l} = \frac{C \cdot b \cdot \left(\frac{\Delta s_{i-1} + \Delta s_i}{2} \right)}{1} = C \cdot b \cdot \left(\frac{\Delta s_{i-1} + \Delta s_i}{2} \right) \quad (11)$$

$$\vartheta_i = \frac{\psi_{i-1} + \psi_i}{2} + \frac{\pi}{2} \quad (12)$$

$$[T_i] = \begin{bmatrix} \cos \vartheta_i & \sin \vartheta_i & 0 & 0 & 0 & 0 \\ -\sin \vartheta_i & \cos \vartheta_i & 0 & 0 & 0 & 0 \\ 0 & 0 & 1 & 0 & 0 & 0 \\ 0 & 0 & 0 & \cos \vartheta_i & \sin \vartheta_i & 0 \\ 0 & 0 & 0 & -\sin \vartheta_i & \cos \vartheta_i & 0 \\ 0 & 0 & 0 & 0 & 0 & 1 \end{bmatrix} \quad (13)$$

$$[k_i] = [T_i]^T \cdot [k_i^*] \cdot [T_i] = \begin{bmatrix} 0 & 0 & 0 & 0 & 0 & 0 \\ 0 & 0 & 0 & 0 & 0 & 0 \\ 0 & 0 & 0 & 0 & 0 & 0 \\ 0 & 0 & 0 & K_{podl,i} \cdot \cos^2 \vartheta_i & K_{podl,i} \cdot \sin \vartheta_i \cdot \cos \vartheta_i & 0 \\ 0 & 0 & 0 & K_{podl,i} \cdot \sin \vartheta_i \cdot \cos \vartheta_i & K_{podl,i} \cdot \sin^2 \vartheta_i & 0 \\ 0 & 0 & 0 & 0 & 0 & 0 \end{bmatrix} \quad (14)$$

2.2 Calculation

In case of major strain when the load decreases, the $\{r\}$ vector cannot be obtained by an explicit solution (1). It is, however, possible to choose strain in a specific point in the construction and look for the corresponding load and the remaining values of the strain. Thus, we obtain a combined task which is described by the equations below.

$$[K] \cdot \{r\} = q \cdot \{\bar{F}\} \quad (15)$$

$$\begin{bmatrix} k_{11} & \cdots & k_{1s} & \cdots & k_{1n_p} \\ \vdots & \ddots & & \ddots & \vdots \\ k_{s1} & & k_{ss} & & k_{sn_p} \\ \vdots & \ddots & & \ddots & \vdots \\ k_{n_p 1} & \cdots & k_{n_p s} & \cdots & k_{n_p n_p} \end{bmatrix} \cdot \begin{Bmatrix} d_1 \\ \vdots \\ w_s \\ \vdots \\ d_{n_p} \end{Bmatrix} = q \cdot \begin{Bmatrix} \bar{F}_1 \\ \vdots \\ \bar{F}_s \\ \vdots \\ \bar{F}_{n_p} \end{Bmatrix} \quad (16)$$

$$\begin{bmatrix} k_{11} & \cdots & \bar{F}_1 & \cdots & k_{1n_p} \\ \vdots & \ddots & \bar{F}_s & & \vdots \\ k_{s1} & & \bar{F}_s & & k_{sn_p} \\ \vdots & \ddots & & \ddots & \vdots \\ k_{n_p 1} & \cdots & \bar{F}_{n_p} & \cdots & k_{n_p n_p} \end{bmatrix} \cdot \begin{Bmatrix} d_1 \\ \vdots \\ -q \\ \vdots \\ d_{n_p} \end{Bmatrix} = -w_s \cdot \begin{Bmatrix} k_{1s} \\ \vdots \\ k_{ss} \\ \vdots \\ k_{n_p s} \end{Bmatrix} \quad (17)$$

$$[K_{\bar{F}}] \cdot \{r_q\} = -w_s \cdot \{K_s\} \quad (18)$$

$$\{r_q\} = [K_{\bar{F}}]^{-1} \cdot (-w_s) \cdot \{K_s\} \quad (19)$$

$\{\bar{F}\}$ - the loading vector induced by a unit load, $q = 1$

$\{K_s\}$ - the vector containing elements in the s^{th} column in the original matrix $[K]$

$[K_{\bar{F}}]$ - the modified rigidity matrix where the s^{th} column is replaced with $\{\bar{F}\}$

$\{r_q\}$ - the modified strain vector where w_s is replaced with the negative value, q

The strain is calculated by iteration unless the required accuracy, ε , is obtained. The accuracy is given by the loads in two subsequent k^{th} iterations.

$$\varepsilon = \left| \frac{(q_k - q_{k-1})}{q_k} \right| \quad (20)$$

In each iteration step, the elements in the rigidity matrix, $[K]$, are re-calculated over and over again. The new values depend not only on changes in the geometry of the construction, but also on changes in the bending rigidity of the individual segments, EI . In each iteration step it is necessary to check whether no tension appears in the hinged rods which replace the passive forces. The tension hinged rods are neglected in creation of the rigidity matrix, $[K]$, because the tension forces cannot, in general, occur in reinforcement contact points. In order to decide whether the tension occurs there, it is necessary to confront the displacement angle of the hinged rod, ϑ_i , and direction of deformation, α_{δ_i} , in the i^{th} joint. If the condition (21) is fulfilled the reinforcement does not deform "into the rock", the reinforcement is not in contact with the rock and no passive forces occur in the i place.

$$\vartheta_i - \frac{\pi}{2} < \alpha_{\delta,i} < \vartheta_i + \frac{\pi}{2} \quad (21)$$

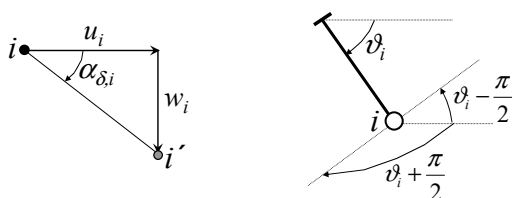


Fig. 4: Graphic explanation to the formula (21)

3 EXAMPLE

The method above was used when processing the 00-0-16/P28 reinforcement in software. The reinforcement consists of three steel arcs which overlap. Fig. 5 shows dimensions of the arcs and overlapping length. Creation of geometry was taken from [1], chapter 2.1. The compressibility of surrounding environment is $C = 36 \text{ MPa/m}^3$ along the perimeter of the reinforcement. The reinforcement is loaded with a continuous vertical even load.

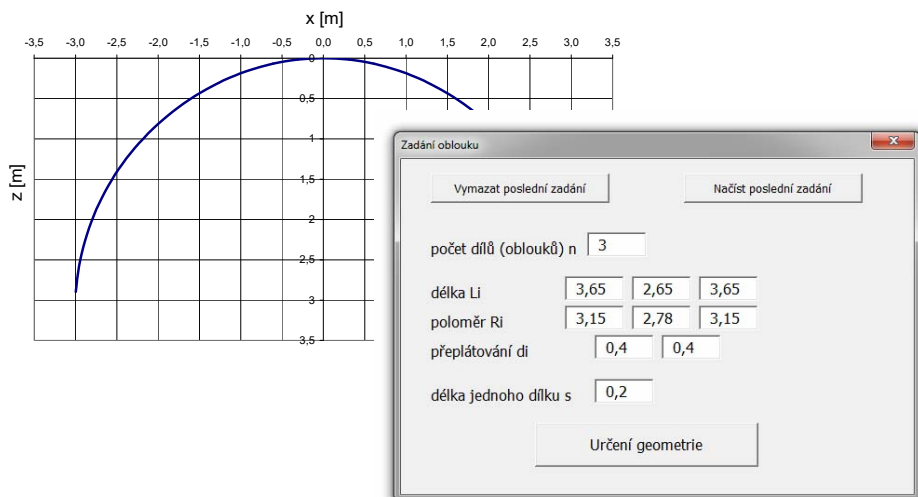


Fig. 5: Geometry of the reinforcement 00-0-16/P-28

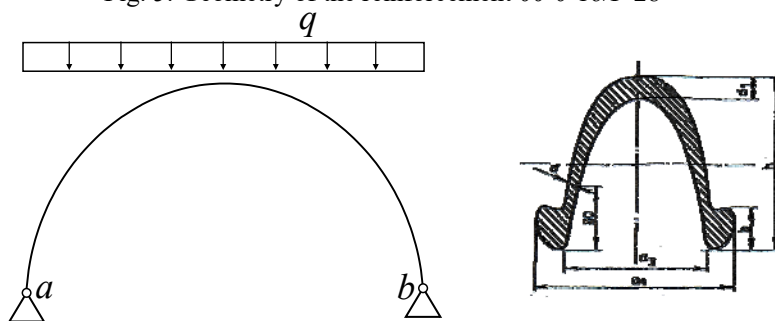


Fig. 6: Loading of the reinforcement and P-28

First, the passive forces were not taken into account in the calculation. Fig. 7 also shows gradual deformation of the reinforcement and the load-deformation curve (q depending on the deformation - vertical dislocation of the arc top, w_s). The load, q , does not exceed 70 kN/m there.

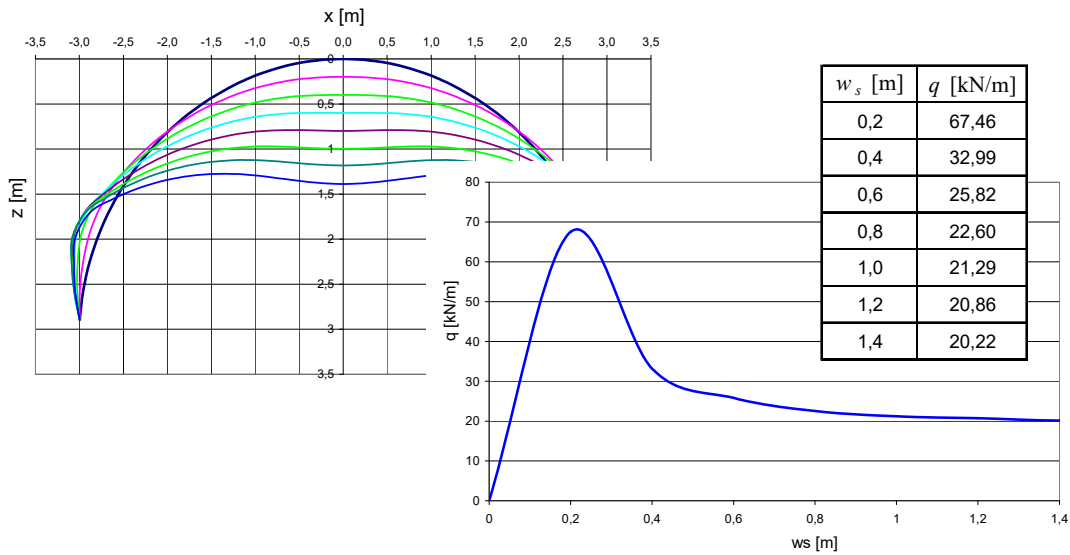


Fig. 7: Gradual loading of the reinforcement, if passive forces do not exist

Then, the passive forces were taken into account in the calculation. Fig. 8 shows behaviour of the reinforcement subject to deformation. In case of major deformation, the rock does not co-act with the reinforcement, and the reinforcement starts deforming “out of the rock”. In this case, the hinged rods which represent the passive forces are not considered in the rigidity matrix $[K]$.

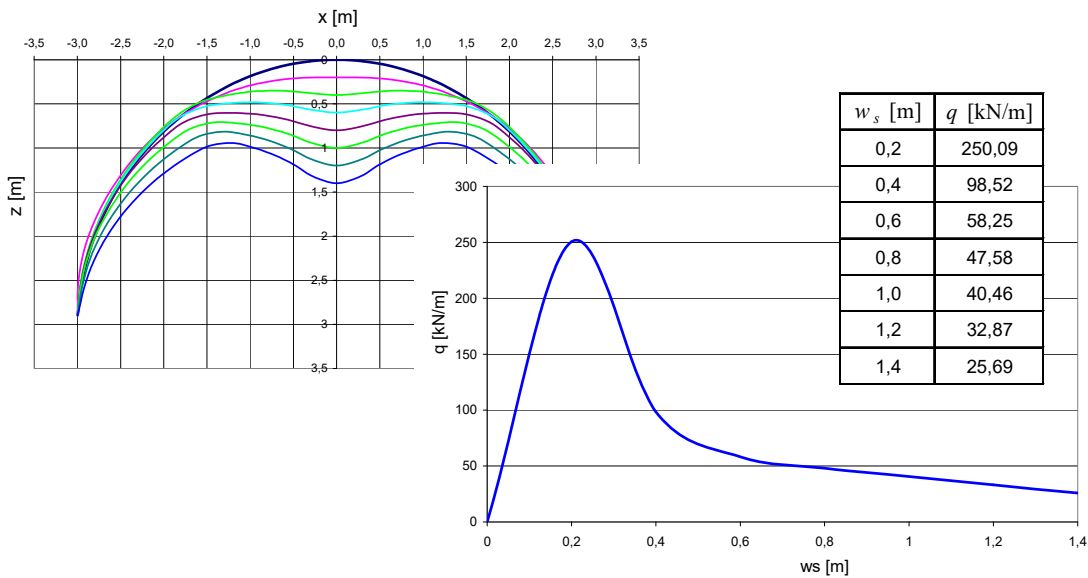


Fig. 8: Gradual loading of the reinforcement, if passive forces exist

More extensive loading is needed to create much deformation, if the passive forces exist. Fig. 8 shows dependence of the loading, q , on the vertical dislocation of the arc peak, w_s .

4 CONCLUSION

In the software, it is possible to determine approximately the working stress-strain characteristics of the steel arc reinforcement, this means the dependence between the deformation and loading with various distribution of the loading forces. The software takes into account the geometric and physical nonlinearity as well as potential rock-reinforcement interaction. It follows from the example above that the load-carrying capacity of the same reinforcement might be very different and depends, in particular, on distribution of active forces affecting the reinforcement and conditions existing for the rock-reinforcement interaction.

ACKNOWLEDGEMENT

This project has been completed thanks to the financial contribution of state funds provided by the Grant Agency of the Czech Republic. The registration number of this project is 105/08/1562.

REFERENCES

- [1] JANAS, P. *Spolehlivost ocelových výztuží dlouhých důlních děl při rázovém zatížení*. Závěrečná zpráva projektu GA ČR 105/04/0458. Ostrava, 2007.
- [2] KADLČÁK, J., KYTÝR, J. *Statika stavebních konstrukcí II*. Brno, 2001. ISBN 80-214-1648-3.
- [3] RANDÝSKOVÁ, L., JANAS, P. Numerické geometricky nelineární řešení soustavy kruhových oblouků pomocí obecné deformační metody. In *Modelování v mechanice 2010*, Ostrava 18. - 19. 5. 2010. Mezinárodní konference. Sborník příspěvků, Ostrava 2010, s. 59-61. ISBN 978-80-248-2234-1.
- [4] RANDÝSKOVÁ, L., JANAS, P. Geometricky a fyzikálně nelineární řešení ocelových oblouků. In *Structural and Physical Aspects of Civil Engineering 2010*, Štrbské Pleso 24. - 26. 11. 2010. Mezinárodní konference. Sborník příspěvků, Košice 2010, s. 1-8. ISBN 978-80-553-0527-1.
- [5] MARKOPOULOS, A., JANAS, P., PODEŠVA, J. Náhradní ohybová tuhost profilu TH-29. In *New Trends in Statics and Dynamics of Building 2010*, Bratislava 21. - 22. 10. 2010. Mezinárodní konference. Sborník příspěvků, Bratislava 2010, s. 101-102. ISBN 978-80-227-3373-1.

Reviewers:

Prof. Ing. Jiří Šejnoha, DrSc, University of Technology, Thákurova 7, Praha 6.

Doc. Ing. Richard Šňupárek, CSc., Institute of Geonics, Czech Republic Academy of Science, Studentská 1768, Ostrava Poruba.